



Molecular Crystals and Liquid Crystals

Publication details, including instructions for authors and subscription information:

<http://www.tandfonline.com/loi/gmcl20>

Transient Shear Stress Response After Flow Start-up and Flow Reversal in Low Molecular Weight Nematic Liquid Crystals

Alain R. Véron^a & Assis F. Martins^a

^a Department Ciência dos Materiais and CENIMAT, Faculdade de Ciências e Tecnologia, Universidade Nova de Lisboa, Caparica, Portugal

Version of record first published: 31 Aug 2006

To cite this article: Alain R. Véron & Assis F. Martins (2005): Transient Shear Stress Response After Flow Start-up and Flow Reversal in Low Molecular Weight Nematic Liquid Crystals, *Molecular Crystals and Liquid Crystals*, 435:1, 199/[859]-213/[873]

To link to this article: <http://dx.doi.org/10.1080/15421400590955226>

PLEASE SCROLL DOWN FOR ARTICLE

Full terms and conditions of use: <http://www.tandfonline.com/page/terms-and-conditions>

This article may be used for research, teaching, and private study purposes. Any substantial or systematic reproduction, redistribution, reselling, loan, sub-licensing, systematic supply, or distribution in any form to anyone is expressly forbidden.

The publisher does not give any warranty express or implied or make any representation that the contents will be complete or accurate or up to

date. The accuracy of any instructions, formulae, and drug doses should be independently verified with primary sources. The publisher shall not be liable for any loss, actions, claims, proceedings, demand, or costs or damages whatsoever or howsoever caused arising directly or indirectly in connection with or arising out of the use of this material.

Transient Shear Stress Response After Flow Start-up and Flow Reversal in Low Molecular Weight Nematic Liquid Crystals

Alain R. Véron
Assis F. Martins

Department Ciência dos Materiais and CENIMAT, Faculdade de Ciências e Tecnologia, Universidade Nova de Lisboa, Caparica, Portugal

Within the framework of the Leslie–Ericksen theory we develop a unified model for the interpretation the complex shear stress response of tumbling nematics after flow start-up and flow reversal. The model accounts quantitatively for: (i) the damping of the oscillations, the vanishing of the doublet structure and eventually a pronounced decay after flow start-up, and (ii) the progressive reappearance of the oscillations after flow reversal (echo phenomenon). Within this model the loss of director coherence, induced partially by noise and partially by a distribution of velocity gradients, is a significant additional cause of damping. A primary cause (but not sufficient) is the director drift towards the vorticity axis as pointed out by other authors. On the other hand, the reappearance of the oscillation is related to reversibility dictated by the mechanical Leslie–Ericksen equations combined with the velocity gradient distribution.

Keywords: flow reversal; flow start-up; liquid crystals; stress oscillations; transient response

1. INTRODUCTION

Nematic liquid crystals exhibit two kind of distinct behaviours under shear flow according to the relative sign of two Leslie viscosities: either the director adopts a stable direction in the flow (flow aligning) or the director continuously rotates (tumbling). Most low molecular

This work was partly supported by the EU-FEDER and Fundação para a Ciência e a Tecnologia (Portugal) under research project POCTI/CTM/2329/01, and research grant SFRH/BPD/8894/2002 to A. Véron.

Address correspondence to Prof. Assis F. Martins, Department Ciência dos Materiais and CENIMAT, Faculdade de Ciências e Tecnologia, Universidade Nova de Lisboa, Caparica, 2829–516, Portugal. E-mail: asfm@fct.unl.pt

liquid crystals are of the flow-aligning type (8CB is an exception). However, by diluting a small amount of some convenient polymer in these liquid crystals it is possible to “transform” a flow-aligning nematic into a tumbling one [1–5]. Accordingly we have at our disposal relatively simple systems described by the Leslie–Ericksen theory for which the effect of director tumbling on the rheological responses may be readily investigated both experimentally and theoretically.

The most obvious effect of tumbling is the occurrence of oscillations in the shear stress response (actually that constitutes the rheological signature of tumbling). However the complex flow that develops leads to the damping of these oscillations and eventually to an additional pronounced decay as observed at low temperature for 8CB [1,6]. Another interesting effect has been observed with a polymer/5CB mixture [1,2], which consists in the progressive reappearance of the oscillations after flow reversal in such a way that the response is symmetric about the reversal point. In this paper we present a model allowing for a clear understanding of all these features together. The flow between a cone and a plate (the most usual experimental setup) is assimilated to the flow between two parallel plates in the homogeneous regime (i.e. when the flow is homogeneous in planes parallel to the plates). However, in order to capture the complexity of the real flow in a simple way we assume that the homogeneous flow between parallel plates is perturbed by inhomogeneous fluctuations that break down the spatial coherence of the periodic director motion, a feature that plays an important role in our model.

2. HOMOGENEOUS FLOW BETWEEN TWO INFINITE PARALLEL PLATES

We consider the flow of an incompressible nematic fluid enclosed between two infinite parallel plates a distance d apart. The top plate moves parallel to itself with the velocity V along a direction chosen as the x_1 -axis while the bottom plate is at rest. The x_2 -axis is chosen normal to the plates and the x_3 -axis is taken parallel to the vorticity axis. The origin of the co-ordinates is such that the top plate lies at $x_2 = d/2$ and the bottom plate at $x_2 = -d/2$. In the general case $V = V(t)$ is an arbitrary function of time imposed by the experimental protocol. In this work we will consider three protocols: (i) flow start-up, i.e. $V(t) = V_0$ for $t \geq 0$; (ii) flow start-up plus flow cessation, i.e. $V(t) = V_0$ for $0 \leq t \leq t_C$ and $V(t) = 0$ for $t \geq t_C$; (iii) flow start-up plus flow reversal, i.e. $V(t) = V_0$ for $0 \leq t \leq t_R$ and $V(t) = -V_0$ for $t \geq t_R$. In all cases V_0 is an arbitrary constant and $\dot{\gamma}_N(t) = V(t)/d$ is the nominal shear rate. In this section, applying the Leslie–Ericksen theory to

a homogeneous flow and neglecting all inertial terms, we derive a closed equation for the director time evolution and an integral expression for the shear stress independent of the velocity.

The homogeneity of the flow implies $v_{1,1} = v_{3,3} = 0$, which combined with the incompressibility condition implies $v_{2,2} = 0$ and finally $v_2 = 0$ because of the fixed boundary conditions. Accordingly, only the two velocity gradients $v_{1,2}$ and $v_{3,2}$ are allowed in this regime. The balance equation for the forces yields

$$\sigma_{2j,2} = 0 \quad j = 1, 2, 3 \quad (1)$$

where σ_{ij} are the Cartesian components of the stress tensor. For a nematic liquid crystal whose local order is characterised by the director \vec{n} the stress tensor reads

$$\sigma_{ij} = -p\delta_{ij} + \sigma_{ij}^e + \sigma_{ij}^v \quad (2)$$

where p is the pressure and where σ_{ij}^e and σ_{ij}^v denote the components of the Ericksen and the viscous stress tensors, respectively. These tensors are defined by [7,8]

$$\sigma_{ij}^e = -\frac{\partial F}{\partial n_{k,i}} n_{k,j} \quad (3)$$

and

$$\begin{cases} \sigma_{ij}^v = \alpha_1 n_k n_p A_{kp} n_i n_j + \alpha_2 n_i N_j + \alpha_3 n_j N_i + \alpha_4 A_{ij} \\ \quad + \alpha_5 n_i n_k A_{kj} + \alpha_6 n_j n_k A_{ki} \\ N_i = \frac{dn_i}{dt} - W_{ik} n_k \end{cases} \quad (4)$$

where F is the Frank free energy density defined by [8]

$$2F = K_2 n_{i,j} n_{i,j} + (K_1 - K_2) n_{i,i} n_{j,j} + (K_3 - K_2) n_i n_j n_{k,i} n_{k,j} \quad (5)$$

with K_i ($i = 1, 2, 3$) the Frank elastic constants. In Eq. (4) A_{ij} and W_{ij} denote the symmetric and antisymmetric parts of the velocity gradient tensor. On the other hand, the equation describing the time evolution of the director may be written as [7,8]

$$\gamma_1 \frac{dn_i}{dt} = \gamma_1 W_{ik} n_k - \gamma_2 A_{ik} n_k + \gamma_2 A_{pq} n_p n_q n_i + h_i^\perp \quad (6)$$

where

$$\begin{cases} h_i^\perp = h_i - (h_k n_k) n_i \\ h_i = -\frac{\partial F}{\partial n_i} + \frac{\partial}{\partial x_j} \left(\frac{\partial F}{\partial n_{i,j}} \right) \end{cases} \quad (7)$$

and \vec{h} is the so-called molecular field. After inserting Eq. (6) in Eq. (4) we get

$$\sigma_{ij}^v = \sigma_{ij}^A + \sigma_{ij}^h \quad (8)$$

with

$$\sigma_{ij}^A = 2\eta_a A_{ij} + 2B(n_i A_{jk} + n_j A_{ik})n_k + Cn_p n_q A_{pq} n_i n_j \quad (9)$$

and

$$\sigma_{ij}^h = \frac{\alpha_2}{\gamma_1} n_i h_j^\perp + \frac{\alpha_3}{\gamma_1} n_j h_i^\perp \quad (10)$$

The three coefficients η_a , B and C are defined by

$$\begin{cases} \eta_a = \alpha_4/2 \\ B = \alpha_6/2 - \alpha_3\gamma_2/2\gamma_1 = \alpha_5/2 - \alpha_2\gamma_2/2\gamma_1 = (\alpha_5 - \alpha_2)/2 - \alpha_2^2/\gamma_1 \\ C = \alpha_1 + \gamma_2^2/\gamma_1 \end{cases} \quad (11)$$

In the sequel we will be concerned with the two velocity gradients $v_{1,2}$ and $v_{3,2}$, and the two stress components σ_{21} and σ_{23} . According to Eq. (3) we have $\sigma_{21}^e = \sigma_{23}^e = 0$ for a homogeneous flow, i.e. $\sigma_{21} = \sigma_{21}^v$ and $\sigma_{23} = \sigma_{23}^v$. In order to employ a matricial formulation we use the following notations

$$\begin{cases} \sigma_a = \sigma_{21} \\ \sigma_b = \sigma_{23} \end{cases}; \quad \begin{cases} \sigma_a^A = \sigma_{21}^A \\ \sigma_b^A = \sigma_{23}^A \end{cases}; \quad \begin{cases} \sigma_a^h = \sigma_{21}^h \\ \sigma_b^h = \sigma_{23}^h \end{cases}; \quad \begin{cases} \dot{\gamma}_a = v_{1,2} \\ \dot{\gamma}_b = v_{3,2} \end{cases} \quad (12)$$

The general Eq. (9) particularises to

$$\begin{cases} \sigma_a^A = \sigma_a - \sigma_a^h = M_{aa}\dot{\gamma}_a + M_{ab}\dot{\gamma}_b \\ \sigma_b^A = \sigma_b - \sigma_b^h = M_{ba}\dot{\gamma}_a + M_{bb}\dot{\gamma}_b \end{cases} \quad (13)$$

where the matrix coefficients M_{aa} , M_{ab} , M_{ba} and M_{bb} are defined by

$$\begin{cases} M_{aa} = \eta_a + B(n_1^2 + n_2^2) + Cn_1^2 n_2^2 \\ M_{ab} = M_{ba} = (B + Cn_2^2)n_1 n_3 \\ M_{bb} = \eta_a + B(n_2^2 + n_3^2) + Cn_2^2 n_3^2 \end{cases} \quad (14)$$

Inversion of Eq. (13) yields

$$\begin{cases} \dot{\gamma}_a = \frac{M_{bb}}{\det(M)} (\sigma_a - \sigma_a^h) - \frac{M_{ab}}{\det(M)} (\sigma_b - \sigma_b^h) \\ \dot{\gamma}_b = -\frac{M_{ba}}{\det(M)} (\sigma_a - \sigma_a^h) + \frac{M_{aa}}{\det(M)} (\sigma_b - \sigma_b^h) \end{cases} \quad (15)$$

where $\det(M)$ denotes the determinant of the matrix M . It is possible to show that $\det(M)$ must be strictly positive so that the inversion of Eq. (13) is always defined. Integration of Eq. (15) over the coordinate x_2 yields¹

$$\begin{cases} P_{aa}\sigma_a + P_{ab}\sigma_b = (Q_a + \varepsilon_a)\dot{\gamma}_0 \\ P_{ba}\sigma_a + P_{bb}\sigma_b = (Q_b + \varepsilon_b)\dot{\gamma}_0 \end{cases} \quad (16)$$

with

$$\begin{cases} P_{aa} = \left\langle \frac{M_{bb}}{\det(M)} \right\rangle & P_{ab} = -\left\langle \frac{M_{ab}}{\det(M)} \right\rangle \\ P_{ba} = \left\langle \frac{M_{ba}}{\det(M)} \right\rangle & P_{bb} = \left\langle \frac{M_{aa}}{\det(M)} \right\rangle \end{cases} \quad (17a)$$

$$\begin{cases} Q_a = \frac{1}{\dot{\gamma}_0} \left\langle \frac{M_{bb}\sigma_a^h - M_{ab}\sigma_b^h}{\det(M)} \right\rangle \\ Q_b = \frac{1}{\dot{\gamma}_0} \left\langle \frac{-M_{ba}\sigma_a^h + M_{aa}\sigma_b^h}{\det(M)} \right\rangle \end{cases}; \quad \begin{cases} \varepsilon_a = \frac{\langle \dot{\gamma}_a \rangle}{\dot{\gamma}_0} \\ \varepsilon_b = \frac{\langle \dot{\gamma}_b \rangle}{\dot{\gamma}_0} \end{cases} \quad (17b, c)$$

where the symbol $\langle \dots \rangle$ denotes $\frac{1}{d} \int_{-d/2}^{d/2} (\dots) dx_2$, and $\dot{\gamma}_0 = V_0/d$. From the definitions we readily get $\langle \dot{\gamma}_a \rangle = V(t)/d = \dot{\gamma}_N(t)$ and $\langle \dot{\gamma}_b \rangle = 0$. Accordingly we have $\varepsilon_a = 1$ after flow start-up ($V(t) = V_0$) $\varepsilon_a = 0$ after flow cessation ($V(t) = 0$) and $\varepsilon_a = -1$ after flow reversal ($V(t) = -V_0$). On the other hand, we always have $\varepsilon_b = 0$, therefore in the sequel we drop this coefficient. Inversion of Eq. (16) yields

$$\begin{cases} \sigma_a = \frac{P_{bb}(Q_a + \varepsilon_a) - P_{ab}Q_b}{\det(P)} \dot{\gamma}_0 \\ \sigma_b = \frac{-P_{ba}(Q_a + \varepsilon_a) + P_{aa}Q_b}{\det(P)} \dot{\gamma}_0 \end{cases} \quad (18)$$

Finally, for the homogeneous flow the director equation reads

$$\begin{cases} \gamma_1 \frac{dn_1}{dt} = (\gamma_2 n_1^2 - \alpha_2) n_2 \dot{\gamma}_a + \gamma_2 n_1 n_2 n_3 \dot{\gamma}_b + h_1^\perp \\ \gamma_1 \frac{dn_2}{dt} = (\gamma_2 n_2^2 - \alpha_3) n_1 \dot{\gamma}_a + (\gamma_2 n_2^2 - \alpha_3) n_3 \dot{\gamma}_b + h_2^\perp \\ \gamma_1 \frac{dn_3}{dt} = \gamma_2 n_1 n_2 n_3 \dot{\gamma}_a + (\gamma_2 n_3^2 - \alpha_2) n_2 \dot{\gamma}_b + h_3^\perp \end{cases} \quad (19)$$

¹We use the following boundary conditions: $v_1 = 0$ at the bottom plate, $v_1 = V$ at the top plate and $v_3 = 0$ on both plates. Moreover we use the fact that σ_a and σ_b are constant in space according to Eq. (1); that is, they can be put outside the integral over space.

The combination of Eqs. (7), (14), (15), (17), (18) and (19) leads to a closed integro-differential equation for the director. On the other hand, according to Eqs. (14), (17) and (18), the shear stress response $\sigma_{21} = \sigma_a$ becomes a functional of the director profile.

Before closing this section we examine how the equations simplify when the director is assumed to be homogeneous along the x_2 -axis. In this case we have $\sigma_a^h = \sigma_b^h = 0 = 0$, $Q_a = Q_b = 0$ and $\langle M_{\alpha\beta} / \det(M) \rangle = M_{\alpha\beta} / \det(M)$. Accordingly, we get $\det(P)\det(M) = 1$, $P_{aa}/\det(P) = M_{bb}$, $P_{bb}/\det(P) = M_{aa}$ and $P_{ab}/\det(P) = -M_{ab}$. With these relations Eq. (18) yields $\sigma_a = M_{aa}\langle \dot{\gamma}_a \rangle = M_{aa}\dot{\gamma}_N$ and $\sigma_b = M_{ba}\langle \dot{\gamma}_a \rangle = M_{ba}\dot{\gamma}_N$. Finally Eq. (15) yields $\dot{\gamma}_a = \dot{\gamma}_N$ and $\dot{\gamma}_b = 0$. As expected, we retrieve the equations corresponding to a three dimensional homogeneous director.

3. A MODEL FOR THE REAL FLOW BETWEEN CONE AND PLATE

Locally the flow between the cone and the plate is assimilated to the flow between two parallel plates. Moreover we assume that we are in a regime where no roll cells develop, which, in principle, should allow us to apply the results of section 2. However a strict homogeneity of the flow in planes parallel to the plates is probably a too strong assumption. To justify this assertion we may invoke several reasons that may be grouped in two categories, namely, (i) what is predicted by the full Leslie-Ericksen theory but is not known (for example the exact velocity profile in a cone-and-plate) and (ii) what is beyond this theory (defects, noise). To take into account all these effects rigorously is an extremely hard task. It is why we overcome this difficulty by adopting a simpler statistical approach. It is worth remarking that the sizes parallel to the plates are relatively large, which implies the possibility for a variable to be broadly distributed at the scale of the set-up (few centimetres in practice) while being weakly inhomogeneous locally. For that reason we assume that we can divide the sample in columns going from the bottom plate to the top plate of the rheometer and perpendicular to the plates, such that their normal section dimensions are much smaller than the size of the plates and the variations of the relevant quantities in any normal section are negligible. In first approximation the results of section 2 apply within each column.

In this viewpoint we believe that the velocity gradients $\dot{\gamma}_a$ and $\dot{\gamma}_b$ are slightly inhomogeneous in planes parallel to the plates; nevertheless their distribution is assumed to be sharp. According to Eq. (19) the

inhomogeneities of $\dot{\gamma}_a$ (or $\dot{\gamma}_b$) generate a distribution of the director velocity, $d\vec{n}/dt$, at equivalent positions within the columns. This feature entrains a progressive loss of the spatial coherence of the director and a distribution of director profile over columns, which constitutes the key point of our approach. Given that the shear stress at the top of a column is a functional of the director profile within the column, it appears that the measured shear stress will be the average of local periodic contributions whose coherence progressively disappears as well. That constitutes an efficient mechanism for damping the oscillations in the global shear stress response. Since inhomogeneities are now allowed, additional velocity gradients may take values different from zero (but small in front of the primary gradient $\dot{\gamma}_a$) contributing to fluctuations of the director velocity. Finally, noise is another source of inhomogeneities; it should be introduced in the mechanical Leslie–Ericksen equations in a way similar to the Langevin approach to Brownian motion.

Fluctuations cannot appear spontaneously in the equations of section 2, they must be introduced in a somewhat arbitrary way; subsequent comparison with experiments will tell us to what extent the procedure is reliable. There are two ways to introduce fluctuations in a known deterministic equation: (i) by adding a fluctuating term or (ii) by letting an external parameter fluctuate around a given mean value. The case (i) corresponds to the Langevin approach, but such a term cannot be chosen arbitrary, it should be derived from theoretical considerations that are beyond this work. For this reason we choose the second option and we consider the nominal shear rate $\dot{\gamma}_N$ as an external parameter that we allow to fluctuate. Briefly, we assume that the actual director velocity within a column may be correctly described by considering an effective (but not real) nominal shear rate $\dot{\gamma}_N + \delta\dot{\gamma}_N$ for this column, where the fluctuation $\delta\dot{\gamma}_N$ may be static, time dependent or, eventually, stochastic. Given that in the vicinity of the mid plane the director is almost homogeneous along the x_2 -axis, we have $\dot{\gamma}_a \approx \dot{\gamma}_N$ and $\dot{\gamma}_b \approx 0$ (see section 2). Accordingly, we can assume that $\delta\dot{\gamma}_N$ is close to the real fluctuation of $\dot{\gamma}_a$ in the mid-plane. The fluctuation $\delta\dot{\gamma}_N$ being unknown, we take advantage of the large sample size for employing a statistical approach. In other words, we introduce a distribution of nominal shear rates over columns of fluid. Accordingly the measured shear stress will be the average of local shear stress (associated to one column) over the distribution of $\dot{\gamma}_N$; thus we can write

$$\sigma_{eff} = \int \sigma_a[\vec{n}; \dot{\gamma}_N] P(\dot{\gamma}_N) d\dot{\gamma}_N \quad (20)$$

4. TRANSIENT RESPONSE AFTER FLOW START-UP

The integro-differential equation describing the director evolution obtained in section 2 is solved numerically by using a finite-difference explicit scheme. To this end the integrals (Eq. 17) are approximated by discrete sums according to the Simpson method. The materials parameters used in this work are quoted from [9]; for mixtures, a correction according to Brochard's theory [5] has been performed. The shear stress response is calculated for a set of constant values of $\delta\dot{\gamma}_N$, the result is then averaged over a Gaussian distribution for $\delta\dot{\gamma}_N$ with zero mean value and a variance that is used as an adjustable parameter. The fact to consider a static fluctuation while noise may be included in $\delta\dot{\gamma}_N$ does not matter much since both static and stochastic fluctuations produce space decoherence of the director motions in a quasi indistinguishable way. In this case, however, the magnitude of the variance of $\delta\dot{\gamma}_N$ must be seen as indicative only. The initial orientation of the director is slightly out of the homeotropic alignment in order to allow for a non-planar configuration. On the other hand, strong anchoring of the director on the plates is assumed. When the director tumbles in the vicinity of the shearing plane while being strongly anchored to the boundary plates a planar distortion develops. When the distortion becomes sufficiently large the elastic torque drives the director away from the shear plane and after enough time it aligns with the vorticity axis in the most part of the sample. This motion of the director toward the vorticity axis explains a part of the experimentally observed damping, as pointed out by Han and Rey [10].

Figure 1 compares the computed shear stress response of 8CB for the homogeneous (1a) and the inhomogeneous (1b) flow. In the first case the doublet structure persists over many cycles, the damping is complete only when a steady state has been reached and the minima are almost stationary. It is worth noting that these features disagree with experiments [1,6]. Within this model the damping results, for a weak part, from the distortion of the director along the x_2 axis, and, for a strong part, from the director motion toward the vorticity axis. The latter point explains why the complete damping is correlated with the achievement of the steady state. When the flow is inhomogeneous the spatial coherence of the director is lost and a mixing of phase angles between different local contributions in the summation of Eq. (20) arises. As a result the damping is accelerated, the doublet structure vanishes rapidly and the minima increase faster. In this case damping and director motion toward the steady state are much less coupled phenomena. For that reason, we can have a complete damping *before* the steady state has been reached, and this latter

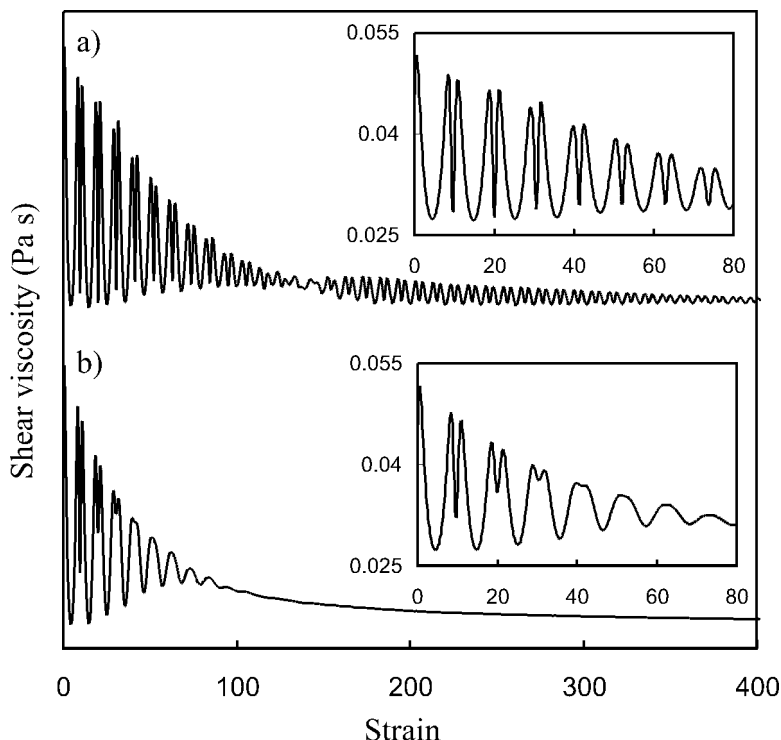


FIGURE 1 Shear viscosity after flow start-up for 8CB at $T - T_{NI} = 4.7^\circ\text{C}$. a) Homogeneous flow ($\delta\dot{\gamma}_N/\dot{\gamma}_N = 0$); b) Inhomogeneous flow ($\delta\dot{\gamma}_N/\dot{\gamma}_N = 3.1\%$).

feature explains the appearance of the ‘additional’ decay observed for 8CB [1]. The fact that such decay is not always observed is only a matter of numerical values for the viscosities. Indeed, the steady value ($t \rightarrow \infty$) of the shear viscosity is close to the Miesovicks viscosity η_a (director aligned with the vorticity axis), so that the observation of a decay will depend on the value of η_a in comparison with the mean value of the first oscillation. In summary, the comparison of figures 1a and 1b clearly shows that the inhomogeneous model agrees with experiment notably better than the homogeneous model. This conclusion is confirmed by Figure 2, where a fit of the inhomogeneous model to experimental data for MSHMA/5CB is shown jointly with a prediction of the homogeneous model for the same parameters. Figure 3 shows clearly how the inhomogeneous model is able to quantitatively account for the progressive vanishing of the doublet structure. It should be pointed out that these two results have been

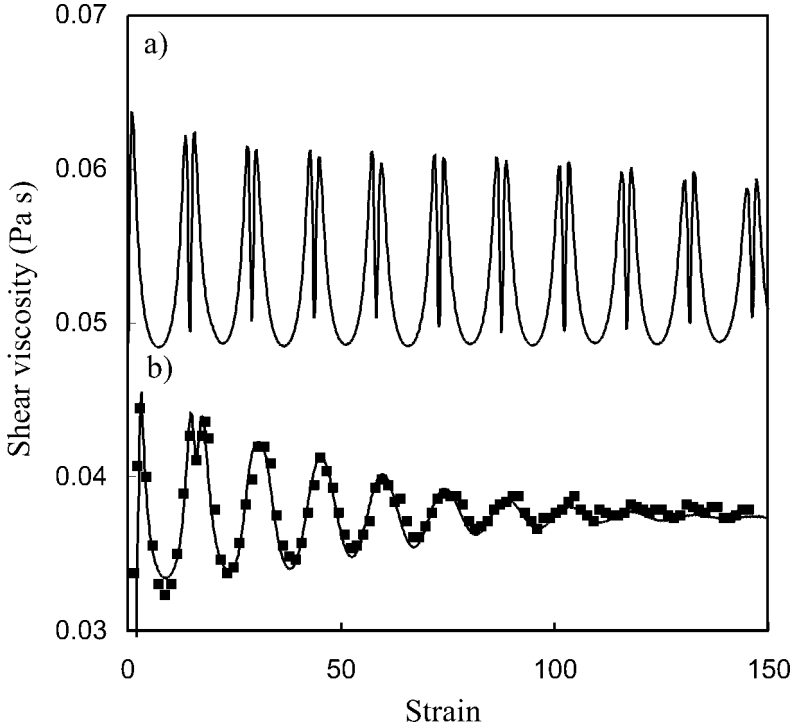


FIGURE 2 Shear viscosity after flow start-up for MSHMA/5CB at $T_{\text{NI}} - T = 10.0^\circ\text{C}$. ■ Experimental data from [3]. — Theoretical curves calculated with $\eta_a = 0.037 \text{ Pa.s}$, $\alpha_3/\alpha_2 = -0.050$, $B = -0.0045 \text{ Pa.s}$, $C = 0.062 \text{ Pa.s}$; a) without fluctuations $\delta\dot{\gamma}_N = 0$; b) with fluctuations $\delta\dot{\gamma}_N/\dot{\gamma}_N = 4.7\%$. The viscosity scale refers to the lower curve; the upper curve is displaced along the ordinate axis, for clarity.

obtained for rather small fluctuations whose relative amplitude, $\delta\dot{\gamma}_N/\dot{\gamma}_N$, was less than 5%, which supports the assumption of weak inhomogeneities; nevertheless their effect is notable.

5. TRANSIENT RESPONSE AFTER FLOW CESSATION AND FLOW REVERSAL

The methodology here is the same as the one presented in section 2; the only difference lies in the new boundary conditions for the velocity after flow cessation or flow reversal (see footnote 1). On the other hand we assume that no sudden change in the director configuration occurs during the sudden change in the flow; that is, the quantities

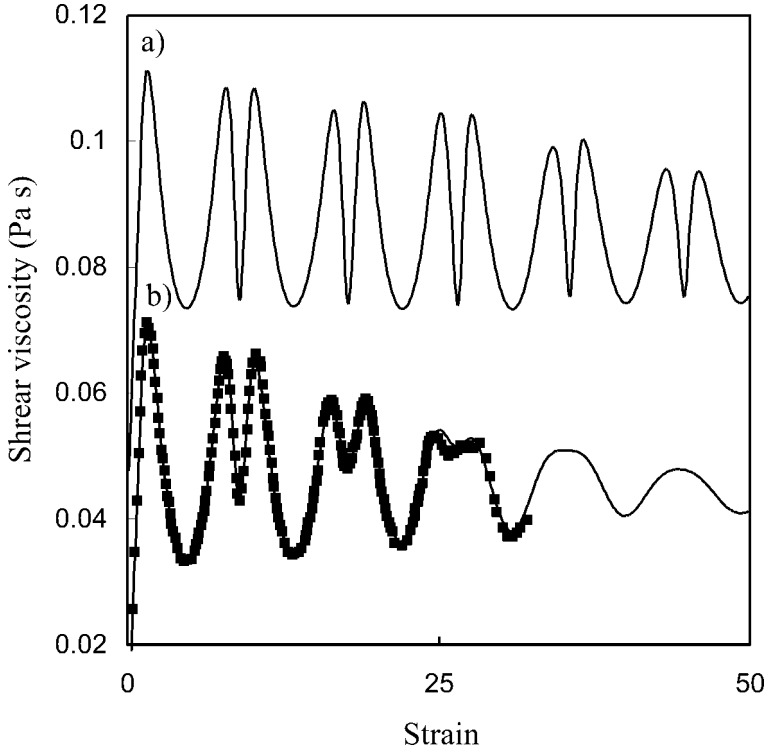


FIGURE 3 Shear viscosity after flow start-up for 8CB at $T_{NI} - T = 4.8^\circ\text{C}$. ■ Experimental data from [3]. — Theoretical curve calculated with $\eta_a = 0.028 \text{ Pa.s}$, $\alpha_3/\alpha_2 = -0.188$, $B = 0.0044 \text{ Pa.s}$, $C = 0.047 \text{ Pa.s}$; a) without fluctuations; b) with fluctuations, $\delta\dot{\gamma}_N/\dot{\gamma}_N = 3.9\%$. The viscosity scale refers to the lower curve; the upper curve is displaced along the ordinate axis, for clarity.

$P_{\alpha\beta}$ and Q_α (see Eq. (17), α and β stand for a or b) are not modified instantaneously. Thus, after flow cessation the shear stress reads (Eq. (18) with $\varepsilon_a = 0$)

$$\sigma_a = \frac{P_{bb}Q_a - P_{ab}Q_b}{\det(P)}\dot{\gamma}_0 \quad (21)$$

If we note σ_{a-} and σ_{a+} the shear stress immediately before and immediately after the sudden change we get

$$\frac{\sigma_{a+}}{\sigma_{a-}} = \frac{P_{bb}Q_a - P_{ab}Q_b}{P_{bb}(Q_a + 1) - P_{ab}Q_b} \quad (22)$$

When the director is free to go away from the shear plane we have $Q_a \ll 1$ and $Q_b \ll 1$ during the process.² These inequalities mean that the elastic contribution to the stress is globally negligible in front of the viscous contribution (see Eqs. (8) to (10)). As a result we get $\sigma_{a+} \ll \sigma_{a-}$; that is, the shear stress drops instantaneously to zero after flow cessation, in agreement with experiments [1]. After flow reversal the shear stress reads (Eq. (18) with $\varepsilon_a = -1$)

$$\sigma_a = \frac{P_{bb}(Q_a - 1) - P_{ab}Q_b}{\det(P)} \dot{\gamma}_0 \quad (23)$$

hence

$$\frac{\sigma_{a+}}{\sigma_{a-}} = \frac{P_{bb}(Q_a - 1) - P_{ab}Q_b}{P_{bb}(Q_a + 1) - P_{ab}Q_b} \quad (24)$$

Thus, when $Q_a \ll 1$ and $Q_b \ll 1$ we get $\sigma_{a+} \approx -\sigma_{a-}$, again in agreement with experiments [1].

As remarked in section 2, when the director is homogeneous in the whole space we have $\dot{\gamma}_a = \dot{\gamma}_N$ and $\dot{\gamma}_b = 0$. As a result, when the flow is reversed at $t = t_R$, i.e. $\mathbf{V}(t) = \mathbf{V}_0$ for $t \leq t_R$ and $\mathbf{V}(t) = -\mathbf{V}_0$ for $t \geq t_R$, $\dot{\gamma}_N$ is changed in $-\dot{\gamma}_N$, hence $d\vec{n}/dt$ is changed in $-d\vec{n}/dt$, because of the linear relation between $d\vec{n}/dt$ and $\dot{\gamma}_N$ (see Eq. (19)). It follows that for $t \geq t_R$ the director goes backward along its past trajectory; more explicitly we have the property $\text{Pr}_1 : \vec{n}(t_R + \tau) = \vec{n}(t_R - \tau)$ for any $0 \leq \tau \leq t_R$. In other words, in the absence of elastic torque the director motion is reversed with flow reversal. It is important to notice that the property Pr_1 holds as soon as the time dependent shear rate satisfies the property $\text{Pr}_2 : \dot{\gamma}_N(t_R + \tau) = -\dot{\gamma}_N(t_R - \tau)$ for any $0 \leq \tau \leq t_R$. The two properties Pr_1 and Pr_2 are fundamental in the formation of an echo. Indeed, let us assume that (i) the (inhomogeneous) fluctuation $\delta\dot{\gamma}_N$ within each column of fluid satisfies the property Pr_2 (such a fluctuation is said reversible) and (ii) at time $t = 0$ the columns of fluid are in the same state (i.e. same director orientation). For $0 \leq t \leq t_R$ each column experiences a different director trajectory because of the inhomogeneous fluctuation $\delta\dot{\gamma}_N$, but for $t_R \leq t \leq 2t_R$ within each column the director goes backward along its past trajectory so that at time $t = 2t_R$ all the columns retrieve their initial configuration. Thus the director coherence that was lost during the first period ($0 \leq t \leq t_R$) is progressively rebuilt during the second period

²It is wrong when the director is constrained to stay in the shear plane; in this case we retrieve the theoretical predictions of Burghardt and fuller [11], but they disagree with experimental data in [1–4,6].

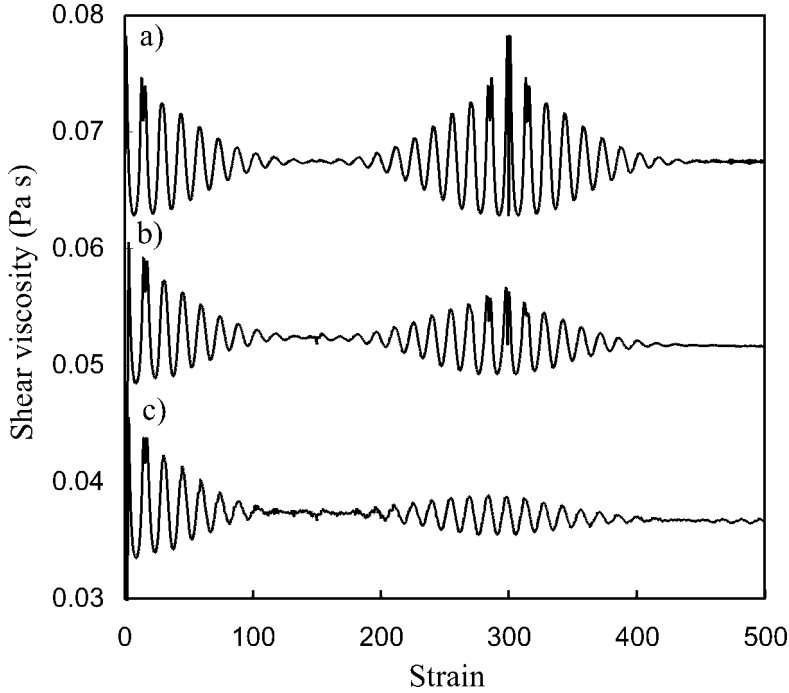


FIGURE 4 Shear viscosity after flow start-up and flow reversal for the mixture MSHMA/5CB. (Leslie viscosities from [5] and [9]). The flow is reversed at $\gamma = 150$. a) Without Frank elasticity, without noise, $\delta\dot{\gamma}_N^r/\dot{\gamma}_N = 4.7\%$ and $\delta\dot{\gamma}_N^s/\dot{\gamma}_N = 0$ b) With Frank elasticity, without noise, $\delta\dot{\gamma}_N^r/\dot{\gamma}_N = 4.7\%$ and $\delta\dot{\gamma}_N^s/\dot{\gamma}_N = 0$ c) With Frank elasticity, with noise, $\delta\dot{\gamma}_N^r/\dot{\gamma}_N = 4.7\%$ and $\delta\dot{\gamma}_N^s/\dot{\gamma}_N = 2.2\%$. The viscosity scale refers to the lower curve; the upper curves are displaced along the ordinate axis, for clarity.

($t_R \leq t \leq 2t_R$). It follows a progressive reappearance of the oscillations in the effective shear stress that moreover is perfectly symmetric about the reversal time. In reality, however, Frank elasticity tends to deteriorate the reversibility of the director motion, i.e. the property Pr_1 is not rigorous. Accordingly, the coherence is not perfectly rebuilt and the amplitude of the echo is smaller than the amplitude of the first oscillation; for the same reason the initial doublet structure is not perfectly retrieved. This situation is still optimal as long as the property Pr_2 is assumed because in reality noise violates Pr_2 . On the other hand, a fully noisy fluctuation $\delta\dot{\gamma}_N$ frustrates the coherence rebuilding. For these reasons we assume that the fluctuation $\delta\dot{\gamma}_N$ may be decomposed in two parts as $\delta\dot{\gamma}_N(t) = \delta\dot{\gamma}_N^r(t) + \delta\dot{\gamma}_N^s(t)$ where $\delta\dot{\gamma}_N^r$ satisfies Pr_2

and $\delta\dot{\gamma}_N^s(t)$ is stochastic; accordingly, we have $\delta\dot{\gamma}_N(t_R + \tau) = -\delta\dot{\gamma}_N^r(t_R - \tau) + \delta\dot{\gamma}_N^s(t_R + \tau)$ for any $0 \leq \tau \leq t_R$ and no relation exists between $\delta\dot{\gamma}_N^s(t_R + \tau)$ and $\delta\dot{\gamma}_N^s(t_R - \tau)$. Therefore, noise entrains an additional loss of echo intensity. All these features are shown in Figure 4. To build this figure the calculations have been performed adding to each term $\delta\dot{\gamma}_N^r$ a stochastic sequence $\delta\dot{\gamma}_N^s(t)$ generated numerically.

This analysis points out the fact that occurrence of reversible inhomogeneities are necessary in order to get an echo. On the other hand it suggests that a quantitative analysis of the echo decay with increasing delay t_R should inform about the relative contributions of noise and reversible fluctuations to the global fluctuation. Note that the effect of the elasticity may be reduced by increasing the distance between the plates, which should make it easier to evaluate the amount of noise in the system.

6. CONCLUSION

Neglecting the inertial terms and assuming a homogeneous flow, we obtained a system of equations for the director and the stress components σ_{21} and σ_{23} . We accounted for slight inhomogeneities in directions parallel to the plates by adding a fluctuation to the nominal shear rate and by adopting a statistical approach. We showed that the inhomogeneous model is able to capture the details of the shear stress response after start-up notably better than the homogeneous model. An important fact is the inability of the homogeneous model to account for the echo phenomenon so that this feature may be seen as an evidence for the occurrence of (reversible) inhomogeneities. An important result is the necessity to introduce a partially reversible fluctuation after flow reversal in order to get the echo. The origin of this fluctuation is not clear; one might conjecture that it is related to an unknown deterministic velocity profile. Two features attenuate the echo intensity with increasing delay: they are the elastic torque and the occurrence of noise. It appears that a quantitative analysis of the echo should allow estimating the magnitude of noise occurring in the system.

REFERENCES

- [1] Gu, D.-F., Jamieson, A. M., & Wang, S.-Q. (1993). *J. Rheol.*, 37, 985–1001.
- [2] Gu, D.-F. & Jamieson, A. M. (1998). *J. Rheol.*, 42, 603–619.
- [3] Gu, D.-F. & Jamieson, A. M. (1994). *Macromolecules*, 27, 337–347.
- [4] Yao, N. & Jamieson, A. M. (1998). *Macromolecules*, 31, 5399–5406.
- [5] Brochard, F. (1979). *J. Polym. Sci.: Polym. Phys. Ed.*, 17, 1367–1374.

- [6] Gu, D.-F. & Jamieson, A. M. (1994). *J. Rheol.*, 38, 555–571.
- [7] Leslie, F. M. (1968). *Arch. Rat. Mech. Anal.*, 28, 265.
- [8] de Gennes P. G. & Prost, J. (1993). *The Physics of Liquid Crystals*, 2nd ed., Oxford University Press: New York.
- [9] Kneppe, H., Schneider F., & Sharma, N. K. (1981). *Ber. Bunsenges. Phys. Chem.*, 85, 784; Kneppe, H., Schneider F., & Sharma, N. K. (1982). *J. Chem. Phys.*, 77, 3203; Karat P. P. & Madhusudana, N. V. (1977). *Mol. Cryst. Liq. Cryst.*, 40, 239–245.
- [10] Han, W. H. & Rey, A. D. (1994). *J. Rheol.*, 38, 1317–1334; Han, W. H. & Rey, A. D. (1995). *J. Rheol.*, 39, 301–322.
- [11] Burghardt W. R. & Fuller, G. G. (1990). *J. Rheol.*, 34, 959–992.